Journal of Catalysis 269 (2010) 122–130

Contents lists available at ScienceDirect

Journal of Catalysis

journal homepage: www.elsevier.com/locate/jcat

Zeolite H-USY for the production of lactic acid and methyl lactate from C_3-sugars

Ryan M. West [a], Martin Spangsberg Holm [b], Shunmugavel Saravanamurugan [b], Jianmin Xiong [b], Zachary Beversdorf [c], Esben Taarning [d,*], Claus Hviid Christensen [d]

[a] University of Wisconsin-Madison, Department of Chemical and Biological Engineering, Madison, WI 53706, USA
[b] Center for Sustainable and Green Chemistry, Department of Chemistry, Technical University of Denmark, DK-2800 Lyngby, Denmark
[c] Iowa State University, Department of Chemical and Biological Engineering, Ames, IA 50011, USA
[d] Haldor Topsøe A/S, Nymøllevej 55, DK-2800, Denmark

ARTICLE INFO

Article history:
Received 4 June 2009
Revised 21 October 2009
Accepted 24 October 2009
Available online 25 November 2009

Keywords:
Lactic acid
Methyl lactate
H-USY
Zeolite
Dihydroxyacetone
Glyceraldehyde
Triose sugar
Deactivation
Biomass

ABSTRACT

Lactic acid is an interesting platform chemical with many promising applications. This includes the use as a building block for the production of biodegradable plastics and environmentally friendly solvents. A study of the liquid-phase conversion of the triose-sugars, glyceraldehyde and dihydroxyacetone directly to methyl lactate and lactic acid catalyzed by inexpensive commercially available zeolites is presented. One particular zeolite, H-USY (Si/Al = 6) is shown to be quite active with near quantitative yields for this isomerization. Deactivation of the H-USY-zeolite was studied by correlating the catalytic activity to data obtained by TPO, XRD, N_2-sorption, and NH_3-TPD on fresh and used catalysts. Coking and irreversible framework damage occurs when lactic acid is produced under aqueous conditions. In methanol, methyl lactate is produced and catalyst deactivation is suppressed. Additionally, reaction rates for the formation of methyl lactate in methanol are almost an order of magnitude higher as compared to the rate of lactic acid formation in water.

1. Introduction

Lactic acid is currently emerging as a building block in a new generation of materials such as biodegradable plastics and solvents [1–3]. These new materials can be produced from biomass-derived precursors and have the potential to replace existing petroleum-based materials by displaying comparable and even superior properties [4]. Lactic acid also has the potential to become a central chemical feedstock for the chemical industry in the production of acrylic acid, propylene glycol, and different useful condensation products [5–8].

However despite its high potential, the major obstacle in a wider implementation of lactic acid-based materials and a lactic acid platform in the chemical industry is the high cost associated with the expensive and cumbersome manufacturing route of lactic acid. The large-scale production of lactic acid relies on the batch-wise fermentation of aqueous glucose under anaerobic conditions [9,10]. The fermentation reaction typically takes 2–4 days and requires calcium hydroxide to be added continuously to maintain a neutral pH-level in order for the bacteria to function optimally, thereby resulting in the formation of calcium lactate. Crystallization of calcium lactate, followed by acidification with sulfuric acid releases the crude lactic acid and gypsum. Typically, one ton of gypsum is formed for every ton of lactic acid produced [1]. Further purification of lactic acid is done by esterification to methyl lactate followed by distillation and hydrolysis to release pure lactic acid.

Lactic acid is an isomer of the triose sugars dihydroxyacetone (DHA) and glyceraldehyde (GLA). The relative stability of the three isomers are in the order of lactic acid ≫ DHA > GLA. The triose sugars can be formed by aerobic oxidation of glycerol using both homogeneous and heterogeneous catalysts [11–14] or by fermentation of glycerol using the *Gluconobactor suboxydans* strain [15–18].

Homogeneous catalysts such as sulfuric acid and sodium hydroxide are known to catalyze the isomerization of DHA and GLA in very hot water (250–300 °C) to give low yields of lactic acid [19,20]. A more effective isomerization catalyst is zinc sulfate, which is reported to give a 75–86% yield of lactic acid in 300 °C hot water [21]. However, the use of a homogeneous isomerization catalyst is problematic from an environmental point of view and the purification of lactic acid can be problematic. Furthermore, the use of very hot water as the reaction media requires expensive pressure resistant equipment which will make a large-scale process unattractive. Homogeneous metal chlorides are active in this isomerization–esterification reaction. In particular, tin

* Corresponding author.
E-mail address: esta@topsoe.dk (E. Taarning).

0021-9517/$ - see front matter © 2009 Elsevier Inc. All rights reserved.
doi:10.1016/j.jcat.2009.10.023

chloride has been found to be able to form methyl lactate in a high 89% yield [22]. However, a high catalytic amount (10 mol%) of tin chloride is used in this case.

Currently, very limited work has been done using acidic zeolites for the conversion of biomass to value added chemicals. Acidic zeolites have been demonstrated to catalyze the conversion of DHA in ethanol to form ethyl lactate, although in a moderate 65% yield [23]. Very recently Lewis acidic beta zeolites were shown to be highly active in the isomerization reaction of DHA and GLA with excellent selectivity toward methyl lactate/lactic acid [24]. These hydrophobic zeolites were made by incorporating Ti, Zr, and Sn into the framework. In particular the Sn-Beta zeolite appears to be an exceptionally promising catalyst in the DHA/GLA conversion. However, application may be limited due to long synthesis time and to the use of tin. Thus an investigation using commercially available solid acids, mainly zeolites containing only silicon and aluminum and sulfated zirconia was undertaken in batch reactors. The most promising of these catalysts, the proton form of an ultra stable Y-zeolite with a Si/Al = 6 (H-USY-6) showed very good activity with near quantitative yields at appropriate conditions. This zeolite was tested under continuous flow within a plug flow reactor to determine the kinetics of the isomerization network and to study the deactivation of the system. A discussion of the catalytic behavior is coupled to the results from XRD, NH_3-TPD, N_2-sorption, FT-IR, and TPO of the fresh and spent zeolite.

2. Experimental

2.1. Chemicals

Dihydroxyacetone (97%), pyruvic aldehyde dimethyl acetal (PADA) (97%), glyceraldehyde (95%), anhydrous pyridine (99.8%), and methanol (99.9%) were purchased from Sigma-Aldrich. Methyl lactate (97%) was obtained from Fluka. Pyruvic aldehyde (PA) was obtained from SAFC Supply as a 40 wt.% aqueous solution while lactic acid was obtained from Fluka and Riedel-de Haën. All the commercially available zeolites used throughout this study were kindly provided by Zeolyst International. The zeolites are pure and do not contain any binder material. Some of the zeolites were received in the NH_4-form. In these cases the zeolites were calcined at 550 °C in air for 6 h prior to use in order to produce the acidic form.

2.2. Catalytic tests

Batch experiments were performed in an Ace pressure tube with magnetic stirring. In these runs, 80 mg of catalyst, 1.25 mmol of substrate (calculated as monomer), and 4 g of water or methanol were added and mixed in the pressure tube using magnetic stirrer ring. The ace pressure tube was then dipped into an oil bath having a temperature of 140 °C for experiments with water and 120 °C for experiments with methanol. The internal temperature during reaction as recorded with an internal thermocouple was 125 °C and 115 °C, respectively.

In the flow reactor set-up, the feed was introduced into the system by either a Waters 501 HPLC pump, or by a Knauer *K-120* HPLC pump. The catalyst was held in place in a stainless steel reactor tube by quartz wool on both sides of the catalyst. The reactor tube was heated by a Carbolite oven while a type E thermocouple attached to the external surface of the reactor tube was used to monitor the reactor temperature. The effluent was collected in a stainless steel collector tube. The system was pressurized to 20 bar of pressure with Argon before each run. Feeds were created by placing a measured amount of substrate in a volumetric flask and filling to the set volume. For concentrated solutions, the mixtures were heated to 69 °C under stirring for 1–2 h to help dissolve the substrate.

Effluent concentrations for batch and flow experiments were characterized by an Agilent 1200 Series HPLC with an R.I. detector and a Biorad Aminex HPX-87H column and an Agilent 6890N GC with an HP-5column and an FID detector. Species were quantified with standards and confirmed with GC-MS, Agilent 6850 GC system coupled with Agilent 5975 C MSD.

2.3. Zeolite characterization

The degree of carbon deposition on used catalysts was determined using temperature-programed oxidation (TPO). Prior to analysis the used zeolites were dried at 110 °C. The TPO was carried out by heating a premeasured amount of used catalyst to 650 °C at 3.5 °C min^{-1} in a gas flow of 20 mL min^{-1} consisting of 5% oxygen in helium. The release of CO and CO_2 was quantified using a BINOS detector. The TPO data are shown in Table 4 as the weight percent of carbon present on the coked catalyst.

NH_3-TPD, N_2-sorption, and XRD were performed on calcined catalyst samples. The procedures used were either as described for the TPO or calcination at 550 °C for 4 h in static air, heated at a ramp of ~2 °C/min. Nitrogen physisorption was measured on a Micromeretics ASAP 2020 after the samples had been degassed in vacuum at 300 °C for 2 h.

Powder X-ray diffraction (XRD) patterns were recorded on a Bruker AXS powder diffractometer. The XRD data are shown in Table 4 as a relative crystallinity, calculated by integrating the peak area of eight characteristic reflections and comparing to the unused zeolite. The reflections used along with the respective 2θ values given in parenthesis were 331 (15.97), 511 (19.01), 440 (20.71), 533 (24.06), 642 (27.52), 822 (31.29), 555 (31.95), and 664 (34.69) [25].

NH_3-TPD measurements were performed on a Micromeritics Autochem II equipped with a TCD detector. Dry weights of the samples were found after evacuation at 300 °C for 1 h. After saturation with ammonia, the weakly bound ammonia was desorbed prior to measurement at 150 °C for 1 h in a He flow of 25 mL min^{-1}. The desorption curve was then attained at a heating ramp of 15 °C per minute to 550 °C at a He flow rate of 25 mL min^{-1}.

FT-IR operated in transmission mode was used to analyze the zeolites on a BioRad FTS 80 spectrometer equipped with a MCT detector. Self-supporting wafers of the zeolites were pressed and were prior to analysis dehydrated under evacuation at 400 °C for 4 h. The absorbance spectra were obtained after the samples were allowed to cool to RT. Pyridine adsorption was done by saturating the zeolite at RT and subsequently heating the sample to 200 °C for 30 min under evacuation. The sample was once again allowed to cool to RT before the spectrum was recorded.

3. Results and discussion

3.1. Reaction pathway

We have investigated the isomerization of the two three-carbon sugars dihydroxyacetone (DHA) and glyceraldehyde (GLA) into methyl lactate and lactic acid over an acidic zeolite catalyst. When the solvent used is methanol, the resulting product becomes methyl lactate and if water is used, lactic acid is formed. Scheme 1 gives the proposed reaction path of the isomerization reaction in either alcohol or water [22–24]. Pyruvaldehyde (PA) is believed to be an initial product formed by the dehydration of DHA/GLA. After addition of water/methanol the resulting hydrate/hemiacetal can isomerize into lactic acid/methyl lactate (path A). The reaction

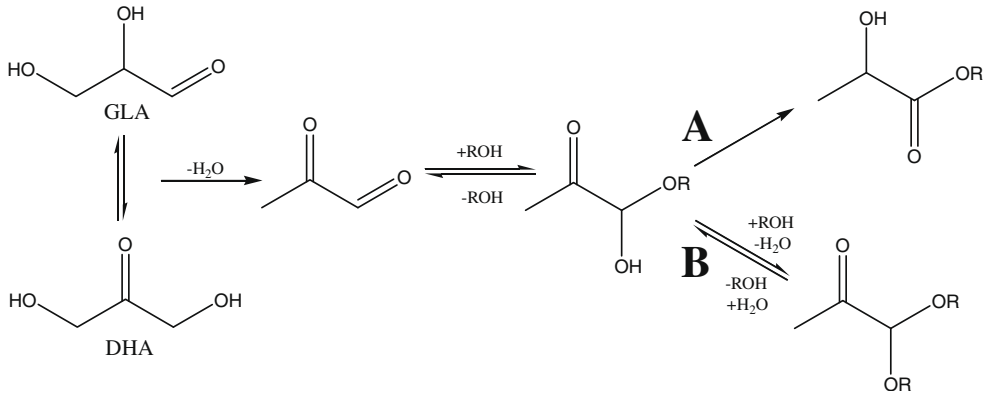

Scheme 1. Reactive pathways of DHA/GLA to lactate/lactic acid (path A) or hydrated/methylated pyruvic aldehyde derivates (path B), in methanol, (R = CH_3) and water (R = H).

path in Scheme 1 will be discussed in detail along with the presentation of the experimental findings.

Product formation in a typical batch experiment was monitored as a function of reaction time. Concentration profiles, based on the carbon balance of the initial triose sugars, are shown in Figs. 1 and 2 for the H-USY-6 zeolite. Fig. 1a and b shows the reaction profiles for DHA and GLA, respectively, in methanol while Fig. 2a and b

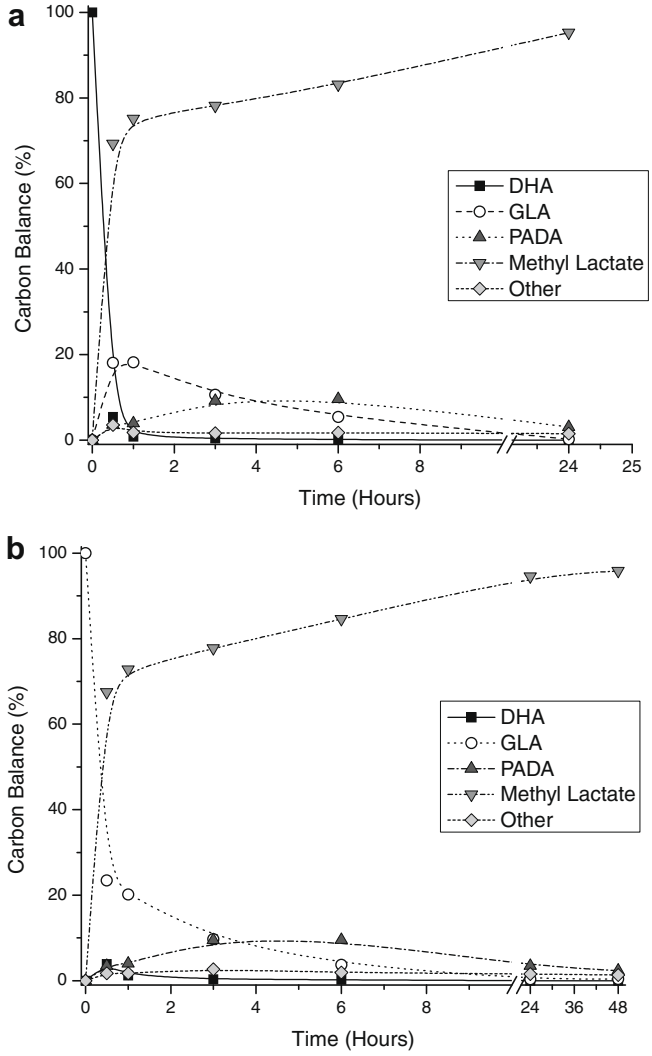

Fig. 1. Batch concentration profiles for DHA and GLA in methanol. Other includes Pyruvic Acid PA, MMP, and TMO. (a) 1.25 mmol DHA in 4.0 g methanol at 115 °C with 80 mg H-USY-6 catalyst; and (b) 1.25 mmol GLA in 4.0 g methanol at 115 °C with 80 mg H-USY-6 catalyst.

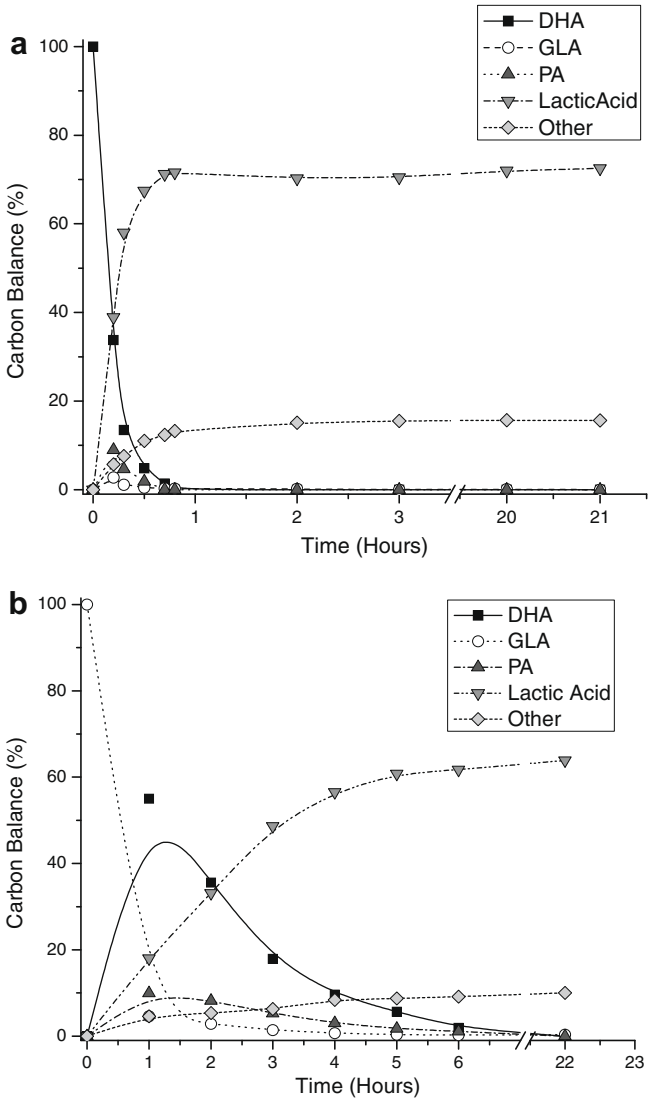

Fig. 2. Batch concentration profiles for DHA and GLA in water. Other includes pyruvic acid, formic acid, acetic acid, levulinic acid, and acetol. (a) 1.25 mmol DHA in 4.0 g water at 125 °C with 80 mg H-USY-6 catalyst; and (b) 1.25 mmol GLA in 4.0 g water at 125 °C with 80 mg H-USY-6 catalyst.

Table 1
Yields obtained from DHA/GLA conversion to lactic acid and methyl lactate over commercial catalysts; 80 mg catalyst, 1.25 mmol substrate (calculated as monomer), 4 g solvent (water or methanol), reaction time 24 h (DHA) or 48 h (GLA), temperature 115 °C (methanol) or 125 °C (water).

Zeolite	Si/Al	Substrate	Water solvent		Methanol solvent	
			Yield of lactic acid (%)	Substrate conversion (%)	Yield of methyl lactate (%)	Substrate conversion (%)
H-USY-6	6	DHA	71	>99	96	99
		GLA	63	>99	98	>99
H-USY-30	30	DHA	47	>99	26	79
		GLA	41	>99	25	64
H-beta	12.5	DHA	63	>99	42	88
		GLA	60	>99	63	90
	19	DHA	37	>99	19	79
		GLA	37	>99	8	64
H-ZSM-5	11.5	DHA	32	>99	17	76
		GLA	30	>99	19	73
	25	DHA	22	>99	7	61
		GLA	23	>99	7	59
H-MOR	10	DHA	39	>99	8	74
		GLA	32	>99	10	28
H-montmorillonite	–	DHA	46	>99	29	44
		GLA	44	>99	30	43
Sulphated zirconia	–	DHA	39	>99	17	96
		GLA	41	>99	37	91
No catalyst	–	DHA	5	>99	0	<0.1
		GLA	4	>99	0	<0.1

shows the profiles in water. The yields of methyl lactate/lactic acid for a variety of solid acids are summarized in Table 1 and are simply the end data point of the individual experiments.

Both GLA and DHA are observed when either substrate is used as a starting reagent as can be seen from Figs. 1a,b and 2a,b. These observations indicate that isomerization between these two sugars occurs and PA is formed as an intermediary product, in accordance with previous reports [26–28]. DHA reacts more quickly than does GLA. In water (Fig. 2b), it is noted that GLA first isomerizes to DHA and the DHA then appears to react. Starting form GLA, the reaction network appears to be dominated by the isomerization and dehydration over the first 6 h. After 6 h, the system approaches the final distribution seen at 22 h. When DHA is instead used as a starting reagent, the final distribution is reached in less than 1 h.

The presence of PA as an intermediate can also be seen in Fig. 2. The concentration of PA is observed to be highest at very short reaction times for both DHA and GLA, thus supporting the hypothesis that PA is an initial intermediate. Addition of either water or methanol forms either hydrated PA or the methyl hemiacetal of PA (PAMA), respectively, both of which can undergo a 1,2-hydride shift and isomerize into lactic acid or methyl lactate (Scheme 1, path A), respectively. The hydrated form of PA can react with an additional water molecule to form the di-hydrated form of PA. It is noted that in water, pyruvaldehyde exists in three forms; aldehyde, hydrated, and di-hydrated with a typical distribution of trace, 56% and 44%, respectively [29]. In the analytical methods used in this study, it was not possible to distinguish these three species, but all are expected to be present. Additionally, the degradation products seen in water consisted of known PA degradation products as seen in commercial sources of pyruvaldehyde, namely pyruvic acid, acetol, and formaldehyde [30].

The same is not true for the methanol case. The PAMA was observed directly as an intermediate species and it can react with another molecule of methanol to form pyruvaldehyde dimethylacetal (PADA), (Scheme 1, path B). PADA has additionally been observed to react further in very small amounts to the methylated form TMP (1,1,2,2-tetramethoxy propane) at low to intermediate conversions. At full conversion, however, PADA, TMP, and PAMA are converted into methyl lactate (Fig. 1) suggesting the back reaction shown in Scheme 1.

3.2. Screening of commercial zeolites

A series of different commercially available zeolites were investigated in the isomerization of the trioses into lactic acid or methyl lactate. Table 1 provides an overview of the yields observed in batch experiments for both GLA and DHA in water and methanol. From Table 1 we conclude that very similar selectivity toward lactic acid/methyl lactate is obtained using either DHA or GLA as the substrate, with only H-beta and sulphated zirconia showing a significant but reproducible selectivity difference with methanol as the solvent.

It is clear from Table 1 that the most effective catalysts for this isomerization–esterification reaction are the proton form of the highly acidic ultra stable Y-zeolite with a Si/Al ratio of 6 (H-USY-6). Indeed, the H-USY-6 zeolite affords methyl lactate yields higher than 95% within the 24 h reaction time which is comparable to the most selective catalysts reported so far in the literature [21–24]. In the absence of a catalyst, DHA and GLA are not converted into methyl lactate/lactic acid in any significant degree. The trioses are stable in pure methanol, but degrade readily in water to form a product mixture consisting of carbonaceous products along with pyruvic aldehyde and some lactic acid. The H-beta zeolite gives moderate yields (DHA 42%/GLA 62%) of methyl lactate, whereas the best H-ZSM-5 catalyst affords only a low yield (<20%) of methyl lactate. In general as the Si/Al ratios are lowered (higher acid density) a higher triose conversion and moderately higher selectivity for methyl lactate is achieved. In a previous work zeolite beta was tested in the isomerization of DHA/GLA to methyl lactate/lactic acid. It was shown that dealumination of zeolite beta by steaming increased the yields of methyl lactate/lactic acid relative to the non-dealuminated catalyst thus indicating that the presence of extra framework aluminum was beneficial for the reaction. However, other factors such as, the effective diffusion rates, acid densities as well as acid strength could also have important roles in determining the activity of the various zeolite structures.

3.3. Characterization by FT-IR

Due to the very large difference in the yield of methyl lactate of the two H-USY samples (98% and 25%, from Table 1) we chose to investigate these two samples by FT-IR using pyridine as a molec-

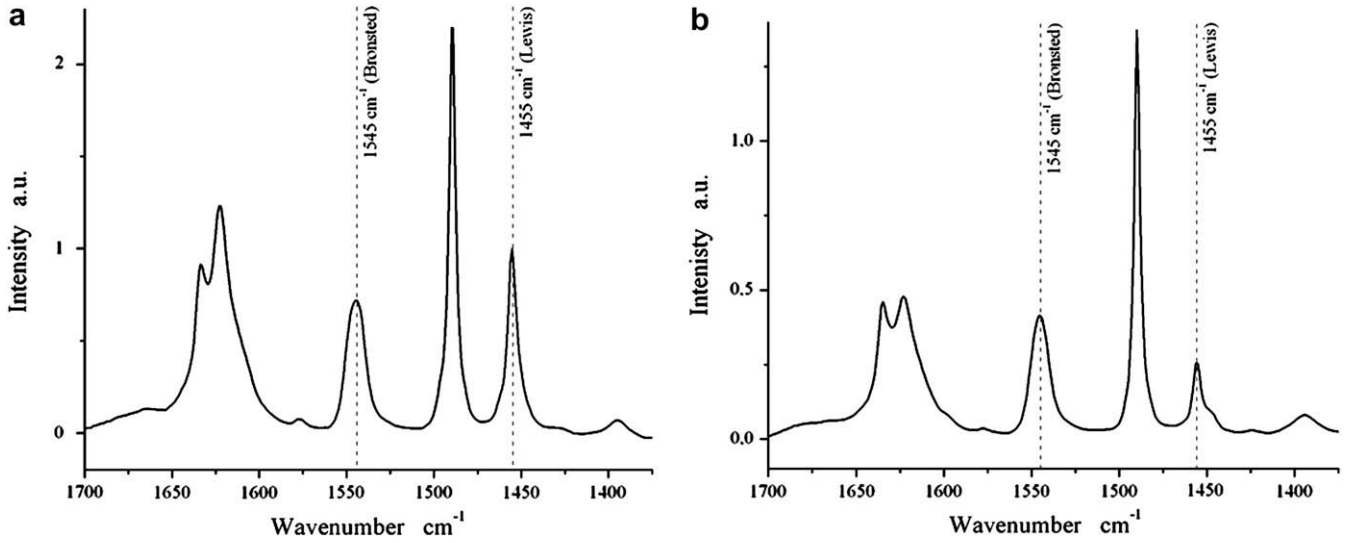

Fig. 3. IR difference spectra after pyridine saturation and subsequent evacuation at 200 °C for 30 min: (a) H-USY-6; and (b) H-USY-30.

ular probe while combined the results with acidity measurements from NH_3-TPD. The dehydrated spectra of the two samples (not shown) reveal the high frequency bridging hydroxyl (HF(OH)) located within the supercage of the zeolite at 3632 cm^{-1}, and the low frequency bridging hydroxyl (LF(OH)) present in the sodalite cage at 3566 cm^{-1} [31]. In addition, contributions at 3602 cm^{-1}, 3526 cm^{-1}, and 3674 cm^{-1} are seen in the case of the H-USY-6 sample. The two former bands located at 3602 cm^{-1} (HF'(OH)) and 3526 cm^{-1} (LF'(OH)) have been reported to occur due to perturbation by extra framework silicoaluminous debris formed upon dealumination of zeolite Y [32,33]. Further, the 3674 cm^{-1} band is said to arise from hydroxyl groups linked to extra framework aluminum (EFAL) species [33]. From pyridine adsorption we were able to differentiate between Lewis and Brønsted acidity while the NH_3-TPD provided a measure of the total acidity. Fig. 3 presents the difference spectra of the pyridine saturated samples after evacuation at 200 cm^{-1} C for 30 min. The relative Brønsted and Lewis acidity ratio could be obtained from integrating the areas under the bands at 1545 cm^{-1} (pyridinium ion) and 1455 cm^{-1} (pyridine) while taking the extinction coefficients into account [34,35]. Using values of $\varepsilon_{Brønsted} = 1.67$ and $\varepsilon_{Lewis} = 2.22$ as reported in Ref. [35], we obtained values of B/L ratio of 1.8 for H-USY-6 and 5.6 for the H-USY-30 zeolite. From NH_3-TPD we found that the total acidity of the H-USY-6 and H-USY-30 samples was 563 $\mu mol/g_{zeolite}$ and 199 $\mu mol/g_{zeolite}$, respectively. Interestingly, these results show that a large fraction of the acidity of the H-USY-6 zeolite actually consists of Lewis acidic sites. Also the total number of Lewis acid sites per gram of zeolite is much larger for H-USY-6 as compared to the H-USY-30 zeolite ($\sim$200 $\mu mol/g_{zeolite}$ and $\sim$30 $\mu mol/g_{zeolite}$, respectively). These findings are in agreement with an earlier report showing that a purely Lewis acidic zeolite beta is highly active for the formation of methyl lactate from triose sugars [24] and they support the hypothesis that the Brønsted and Lewis acidic sites can catalyze two different reaction paths, with only the Lewis acidic sites leading to the formation of lactic acid/methyl lactate in appreciable amounts from DHA/GLA.

3.4. Flow experiments

The high yields obtained when using the H-USY-6 zeolite as catalyst merited further study in continuous flow mode. The stability of the H-USY-6 catalyst at high conversion in water and in methanol was investigated for approximately 45 h on stream. Reaction

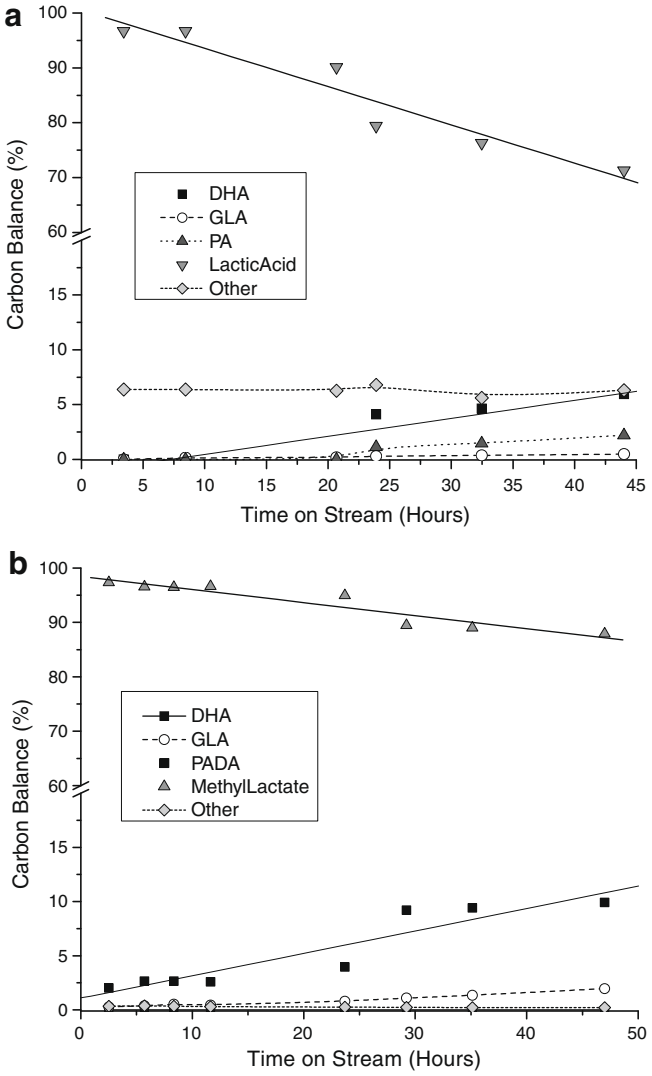

Fig. 4. Concentration profiles vs. time on stream for 0.31M DHA over H-USY-6 catalyst. Other includes pyruvic acid and TMO. (a) DHA conversion in water at 177 °C, WHSV of 0.18 h^{-1}. Other includes pyruvic acid, formic acid, acetic acid, levulinic acid, and acetol; and (b) DHA conversion in methanol at 157 °C, WHSV of 0.16 h^{-1}.

conditions for the two experiments were chosen to achieve full conversion initially, and a high yield of products, i.e. in the case of water, a reaction temperature of 177 °C, concentration of 0.31 M DHA, and a WHSV of 0.18 h^{-1} was chosen, while for methanol a temperature of 157 °C, concentration of 0.31 M DHA, and WHSV of 0.16 h^{-1} was used. Fig. 4 presents the observed product compositions obtained by sampling the effluent as a function of time on stream.

In Fig. 4a while the initial yield of lactic acid in water was quite high, 95%, the sample showed continual deactivation. After around 25 h, the concentration of both unreacted feed and pyruvic aldehyde (PA) increased significantly, while the yield of lactic acid decreased sharply. This deactivation continued for the duration of the run reaching a ~70% yield of lactic acid after 44 h. In the case of methanol as a solvent we observed a much improved stability within the 47 h as shown in Fig. 4b. The yield of methyl lactate remained around or above 90% for the duration of the run. As the yield of methyl lactate drops slowly, the yield of pyruvic aldehyde dimethyl acetal (PADA) increases. Only low concentrations of unreacted triose sugars were observed in the effluent.

3.5. Kinetic study in the flow system

In order to better understand the current system, a simultaneous investigation of the kinetics and deactivation under various reactions conditions were conducted. The temperature, feed concentration, and feed substrates were systematically varied as shown in Table 2 while the catalyst loading was adjusted to keep the initial disappearance of reagent to less than 70% and the yield of lactic acid/methyl lactate to less than 50%. The initial activity and calculated initial activity of the H-USY-6 as a function of systematically altered reaction conditions are shown in Table 2. The initial measured activities are given for the disappearance of triose sugars (total disappearance of GLA and DHA), the appearance of lactic acid/methyl lactate, and for the appearance of intermediate species PA/PAMA (pyruvic aldehyde methyl acetal), and PADA, (depending on the solvents). The calculated values were fit with a simple kinetic model while as described in detail in the modeling section below.

As one would expect, the rates increased as the temperature was increased at otherwise constant conditions, (entries 1–6). The activity of DHA and GLA in water at ~160 °C and 0.31 M (entries 4 and 7) showed quite different results. The total disappearance rate when GLA is the starting reagent is only 305 μmol/(min * g_{cat}), while this value is 425 when DHA is the starting reagent. Likewise, the appearance of lactic acid from GLA is only 120 compared to 355 for DHA at the same conditions. The observation suggests isomerization of GLA to DHA readily occurs with the DHA ultimately reacting as discussed later. When the suspected intermediate species PA is reacted at similar conditions, (entry 8), a higher disappearance of feed of 820 and an appearance of lactic acid of 770 is observed. This observation appears reasonable since the dehydration step is surpassed and the kinetics of isomerization are quite favorable as discussed in a later section.

When the feed concentration of DHA is increased at any temperature, the disappearance of triose sugars is seen to likewise increase (entries 2, 9, and 10 and entries 4, 11, and 13). However, the appearance of lactic acid is not observed to increase correspondingly. In Table 1, it is noted that when given enough time, complete conversion of triose sugars to products other than lactic acid is possible without catalyst in water. It is believed that similar degradation reactions are occurring when the concentration of feeds is increased beyond 0.31 M.

Switching the solvent to methanol (entries 14–19) caused a drastic difference in the observed rates. For a 1.25 M feed solution of DHA, the initial disappearance of triose sugars increased by a factor of ~7 from 775 in water at 160 °C (entry 11) to 5590 in methanol at 150 °C (entry 18), while the appearance increased by a factor of ~8 from 405 for lactic acid to 3315 for methyl lactate. A similar trend is seen at 130 °C where the rate of disappearance increases from 225 to 1305, while the rate of appearance increases from 50 to 1060 (entries 2 and 15, respectively).

Interestingly, using a mixed solvent of methanol and water (entry 17) produced disappearance and production rates between that of pure methanol and water. For a 1.25 M solution of DHA, a 45/55 molar mixture of methanol and water (64.5 wt.% methanol) at 150 °C showed a disappearance rate of 1300, double that of pure water, 775 (entry 11), but much less than that of pure methanol, 5590 (entry 18). The rate of appearance of product, a mixture of lactic acid and methyl lactate for the 45/55 mixture was 860, again about double that of pure water, 405, and much less than that of pure methanol 3315. A mixture of the solvents is indeed an interesting situation since for every one mole of DHA reacted, one mole of water is created in an alcohol solvent meaning that minor

Table 2
Initial rates of reaction under systematically varied conditions using H-USY-6. The total number of acid sites are 563 umol/g based on NH_3-deposition. The number of Brønsted and Lewis acid sites corresponds to 362 μmol/g and 200 μmol/g, respectively (based on pyridine IR-adsorption).

Entry	Conditions of run				Measured initial rate (μmol/(min*g_{cat}))				Calculated rate (μmol/(min*g_{cat}))		
	Temp. (°C)	Reagent	Solvent	Concentration (M)	Triose dissappearance	LA/ML appearance	PA/PAMA appearance	PADA appearance	Triose dissappearance	LA appearance	PA appearance
1	116	DHA	Water	0.31	27	17	2		32	23	8
2	130	DHA	Water	0.31	75	50	8		75	40	35
3	142	DHA	Water	0.31	100	100	15		110	65	35
4	165	DHA	Water	0.31	425	355	40		450	315	90
5	172	DHA	Water	0.31	550	445	25		525	380	75
6	190	DHA	Water	0.31	1530	1055	205		1545	1075	230
7	160	GLA	Water	0.31	305	120	30				
8	160	PA	Water	0.36	–	770	820[a]		–	820	930[a]
9	130	DHA	Water	0.80	180	50	30		210	90	110
10	130	DHA	Water	1.25	225	30	45		260	120	130
11	160	DHA	Water	1.25	775	405	125		710	415	240
12	160	PA	Water	1.25	–	780	865[a]		–	855	975[a]
13	160	DHA	Water	3.44	2475	340	405		2480	1495	785
14	112	DHA	MeOH	1.25	735	620	30	45			
15	130	DHA	MeOH	1.25	1305	1060	35	300			
16	130	GLA	MeOH	1.25	1270	800	25	190			
17	150	DHA	MeOH/water	1.25	920	865	95	150			
18	150	DHA	MeOH	1.25	5590	3315	385	1400			
19	165	DHA	MeOH	1.25	10080	4600	905	2850			

[a] Disappearance of PA.

amounts of water are inevitably present. Further, this situation is important if operating in solvents of only technical grade. Importantly as just outlined above using the mixture of water and methanol did increase the rates with respect to those observed in pure water. However, reaction rates in the solvent mixture are still much closer to the rates seen in water than those in pure methanol.

3.6. Deactivation

The reasons for deactivation were investigated by characterizing fresh and used catalysts. Table 4 demonstrates the surface properties for fresh and selected used catalyst collects from Table 3 as well as H-USY-6 zeolites under modeled deactivating conditions. Table 4 entry 1 represents the fresh, unused H-USY-6 zeolite which is used for comparison. Entries 2–8 contains data for the used catalysts and were chosen as to cover the range of reaction times, temperatures, feeds, concentrations, and solvents used.

Entry 2 was tested at low temperature (116 °C) and short time (6 h) on stream while entry 3A corresponds to the zeolite used in Fig. 3a namely a temperature of 177 °C and time on stream 44 h in water. Entry 3B is the same sample without calcination to show the influence of carbon on the surface area. Characterizing the three used zeolites we note that the adsorption characteristic of entry 2 is very similar to the parent zeolite exemplified by a micropore volume which only decreased from 0.253 ml/g to 0.236 ml/g indicating that the zeolite structure is mostly preserved. This is in strong contrast to the prolonged and high temperature reaction used for entry 3A which resulted in an almost complete loss of crystal integrity. This can be seen by a reduction in the measured surface area and micropore volume of around 80%, a loss of acidity of 46% as well as a final crystallinity calculated to <10%. Furthermore, the catalyst is heavily covered in carbon, containing as much as 9 wt.% carbon.

Entry 4 shows data for the zeolite after a time on stream of 47 h at 157 °C in the conversion of DHA in methanol (Fig. 3b). Ammonia-TPD, porosity measurements, and the estimated crystallinity all shows that less framework deterioration takes place during the reaction in methanol compared to water (entry 3A). However, a modest loss in micropore volume, surface area, and acidity is seen along with a decrease in the calculated crystallinity of around 40% indicating that the catalyst has suffered some structural damage in excess of the deactivation by carbon deposits.

Entries 5 and 6 shows that the highest deposition of carbon takes place when PA is used as the feed, (Table 2 entries 8 and 12, respectively). In 9 h at 160 °C, 5.2% of carbon had deposited onto the H-USY-6 zeolite when using a feed of 0.36 M PA as substrate. Increasing the PA concentration aggravates the deposition of carbon, since 15.7% is deposited in only 5 h when a feed consisting of 1.25 M PA was used. In contrast, after running for 44 h, a 0.31 M DHA solution in water amounted to 9.0% carbon. In addition to the excessive carbon deposits, high surface area and micropore volume losses were also observed (entry 5). It is also noted that the deactivation of the catalyst in the two runs using PA as a feed was also the most rapid among all feeds and conditions tested.

Entries 7 and 8 in Table 4 were created by flushing the H-USY-6 zeolite with either a 0.31 M lactic acid solution in water or a 0.31 M methyl lactate solution in methanol overnight at the specified temperature. The lactic acid and methyl lactate were quantitatively recovered in the effluent indicating that the reverse reactions do not occur. These experiments show that the desired end products in methanol and water, methyl lactate and lactic acid, are not the cause for the excessive carbon deposition onto the zeolite. Importantly, we observe that the product in water, lactic acid, strongly damages the catalyst already after 12 h. Again this is in strong contrast to what is observed in the case of methyl lactate in methanol where more modest changes in the structure of the catalyst were detected for the comparable reaction conditions (entries 4 and 8). Although the XRD show a decrease of 41.2% for this sample the effect on micropore volume, surface area and total acidity of the zeolite is much smaller.

The specific cause of irreversible zeolite destruction was further systematically tested under controlled conditions. Entries 9 through 15 were created by exposing the fresh H-USY-6 zeolite to the specified conditions listed in a sealed teflon container rotated at 20 rpm. The zeolite was subsequently recovered by filtration and washed thoroughly with demineralized water and dried before analysis.

Stirring the zeolite in demineralized water for 24 or 48 h at 140 °C (entries 9 and 10) slightly decreased the surface areas and

Table 3
Modeled kinetic parameters for Scheme 1 on H-USY-6.

	Ea (kJ/mol K)	ln(A) (1/mass)
1	53 ± 13	17.4 ± 8.9
2	61 ± 15	20 ± 13
3	89	26

Table 4
Physical properties of fresh, used, and treated H-USY-6 catalysts.

Entry	Temperature (°C)	Solvent	Feed	Concentration (M)	Time (h)	Location	TPO (% C)	BET (m^2/g)	V_{micro} (mL/g)	V_{meso} (mL/g)	S_{meso} (m^2/g)	NH_3-TPD (umol/g)	XRD, C/C_0 (%)
1	–	–	–	–	–	–	–	725	0.253	0.058	134	563	100
2	116	Water	DHA	0.31	6	Reactor	2.0	674	0.236	0.076	142		
3[A]	177	Water	DHA	0.31	44	Reactor	9.0	182	0.048	0.198	97	306	8.6
3[B]	177	Water	DHA	0.31	44	Reactor		115	0.015	0.188	71		
4	157	MeOH	DHA	0.31	47	Reactor	2.7	619	0.217	0.060	128	461	59
5	160	Water	PA	0.36	9	Reactor	5.2	246	0.076	0.102	79		
6	160	Water	PA	1.25	5	Reactor	15.7						
7	177	Water	LA	0.31	12	Reactor	1.7	405	0.129	0.151	127	394	34
8	137	MeOH	ML	0.31	11	Reactor	1.8	708	0.246	0.071	142	486	56
9	140	Water	–	–	24	Vial		555	0.211	0.089	108	561	80
10	140	Water	–	–	48	Vial		554	0.208	0.108	108		
11	140	Water	LA	0.3	2	Vial		716	0.248	0.094	164		
12	140	Water	LA	0.3	8	Vial		670	0.232	0.106	164		
13	140	Water	LA	0.3	24	Vial		537	0.188	0.118	129	490	71
14	140	Water	LA	1	24	Vial	0.4	238	0.017	0.290	223	158	≈0
15	140	MeOH	–	–	24	Vial		693	0.251	0.057	131	486	93

[A] Calcined
[B] uncalcined.

crystallinity of the sample, however it did not markedly decrease the total acidity of the zeolite.

Carefully repeating the experiment by using a 0.3 M solution of lactic acid and a shorter treatment period caused a more pronounced destruction of the zeolite than pure water. Entries 11–14 show the systematic decrease in surface areas, and micropore volume corresponding to treatment times of 2, 8, and 24 h in 0.3 M lactic acid. At 24 h, the surface areas number of acid sites and crystallinity of the sample subjected to 0.3 M lactic acid (entry 13) were all lower than the corresponding values in pure water (entry 9) at 24 h. Further increasing the concentration of lactic acid to 1.0 M (entry 14) caused a complete destruction of the zeolite with no recognizable diffraction peaks present in the XPRD diffractogram, i.e. the crystallinity of this sample was ≈0%. Results from NH_3-TPD and N_2-sorption analysis support the complete dismantling of the zeolite. Importantly, a concentration of approximately 0.3 M of lactic acid, which is the concentration of final product in either the batch or flow experiments, is sufficient to destroy the zeolite suggesting that it is necessary to work with dilute systems if water is used as the solvent. In entry 8 we used anhydrous methanol for the treatment. It is however clear from the results that the zeolite is extremely stable in pure methanol as the zeolite characteristics are practically identical to the fresh zeolite.

As highlighted from the characterization above it is important to distinguish between the reversible deactivation occurring through coking of the zeolite in contrast to the irreversible deactivation through structural damage of the zeolite. The results indicate that coking originates from decomposition of PA and not from the end products. The conditions that lead to the most rapid loss in activity can be summarized as follows. Higher temperatures and higher concentration of lactic acid (either directly or through the formation from PA) are detrimental to the zeolite structure. Using water compared to methanol as a solvent causes a higher level of irreversible damage. This difference arising from the solvent is further increased as lactic acid also causes far more destruction than does methyl lactate. Minimal deactivation through destruction of the zeolite can therefore be expected when operating at low concentrations, low temperature, and when using an alcohol as the solvent.

3.7. Modeling the reaction path

The initial rate of reaction was modeled as a plug flow reactor with a series of simple first order reactions as shown in Scheme 2 for all runs involving DHA and PA with water as a solvent. The forward rate constants were assumed to be Arrhenius expressions of the form, $k_i = A_i \exp^{\frac{E_{Ai}}{RT}}$. The pre-exponential factor A and activation energy of each step were then estimated by integrating over the mass of catalyst in Matlab using the lsqnonlin function to minimize the differences in calculated and experimental rates for the disappearance of trioses, appearance of pyruvaldehyde, and the appearance of lactic acid. The fit parameters for each step are found in Table 3, while the calculated rates are included in Table 2.

Despite fairly good agreement over the large temperature and concentration range of this study, the confidence intervals seen in Table 3 are quite large. This variance is primarily due to relatively good fit over a range of values; that is similar forward rate constants can be calculated with a range of pre-exponential and activation energies. The initial disappearance of triose sugars was less than 70% while the initial yield was less than 50%, hence the model used incorporated the changing concentrations of the reagents through the reactor. This reaction model is not differential and hence the confidence intervals are quite large. Despite these large intervals, several important conclusions can be made by calculating the forward rate constants at the best fit values for each step in Scheme 2. It is observed that the forward rate constant for isomerization is the largest forward rate constant at all temperatures of this study. The ratio of k_2/k_1 increases as the temperature is increased from a value of 1.1 at 115 °C to 1.7 at 190 °C. This higher value for k_2 implies that the isomerization step occurs more readily than the dehydration step and that the isomerization is relatively more favorable as the temperature is increased. A second trend can be seen by comparing the degradation and isomerization constants, k_2/k_3. At 115 °C this value is 14.6, heavily favoring the isomerization. As the temperature is raised however to 190 °C, this ratio drops swiftly to 3.6 indicating that the degradation reactions become much more favorable at higher temperatures.

The model predicts the initial rates for a variety of concentrations, temperatures, and feeds relatively accurate. The differences between the calculated and observed initial rate of disappearance of triose species and pyruvic aldehyde are less than 20% for concentrations ranging from 0.31 M to 3.44 M and temperatures from 116 to 190 °C indicating the system is well described by the assumptions of first order kinetics and simple activation energies. The estimated production rate of lactic acid is also accurately modeled for the tests at low concentration. Deviations between the model and experimental data are largest at high concentrations with the largest differences between the predicted and observed rates occurring for the production of LA in entries 10 (131 °C 1.25 M) and 13 (159 °C 3.44 M). Since the reaction pathway is believed to be a series of reactions, and since the model does not include surface coverage terms, one possible explanation is that the catalytic sites are covered by either initial species DHA or water, and are blocked from reaction of DHA. A second explanation could include a diffusion limitation at high concentration. The surface blocking explanation is better supported, however, by the close fit between experimental and calculated rates when the intermediate species, PA is used. At higher concentrations of PA (entry 12) the rate of lactic acid production is relatively close to the rate of PA disappearance, while the same is not true of DHA at the same conditions (entry 11). If the system was diffusion limited, one would expect large differences for both cases, however if the initial reactivity of DHA is limited, large deviations would only be expected for the case starting with DHA, as observed.

Previous authors have modeled the degradation of triose sugars under isothermal conditions without a catalyst [26,27]. These studies looked at the isomerization and degradation of GLA and DHA into PA. As in the current case, first-order kinetics were found to appropriately model the disappearances of triose sugars and PA. As expected, the heterogeneously catalyzed activation energy

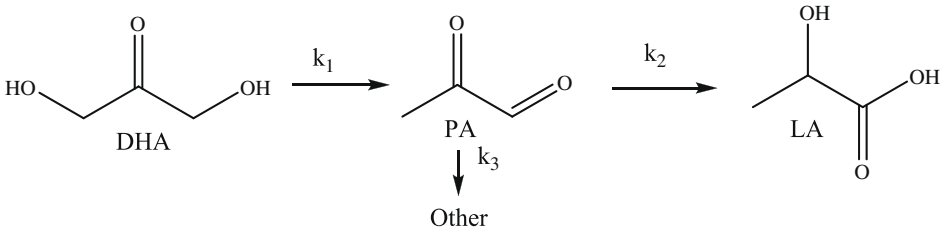

Scheme 2. Modeled reaction scheme for the conversion of DHA into LA.

determined here is much lower than previous reports for the dehydration of triose sugars (53 ± 13 vs. 75–92 kJ/mol, respectively). The degradation/isomerization of PA determined in this report are comparable to previous values, with the isomerization having a lower activation energy (61 ± 15 kJ/mol) and the degradation reaction having similar value (89 kJ/mol) to the other reports (77–94 kJ/mol). It is important to note that due to the aqueous environment of this and previous studies, PA is present as the hydrated and dehydrated forms. This implies that the degradation reactions of PA (as the mono- and di-hydrate) would proceed even in the absence of heterogeneous catalyst and further suggests avoidance by operation at lower temperatures.

From the modeling study, we see that the optimal reactions conditions for the production of a lactic acid derivative are low concentrations in an alcohol solvent such as methanol at low temperatures. The experimental data for the isomerization reactions can despite a relative large confidence interval be described by a series of first-order reaction and the model can be used to gain useful information of the involved rate constants. Specifically, the higher temperatures favor isomerization, k_2 over dehydration k_1, but also favor degradation k_3 over isomerization k_2. To limit degradation to other products, it is therefore suggested that the reaction be run at lower temperatures.

4. Conclusion

It has been demonstrated that the Lewis acidic H-USY-6 zeolite is highly effective for the isomerization of triose sugars to lactic acid and methyl lactate. Indeed, methyl lactate can be formed in almost quantitative yields directly from DHA and GLA, using this inexpensive zeolite. The transformation can be modeled via a series of first order reactions in water. In methanol, the rate of reaction is as much as an order of magnitude higher than in water. The catalyst deactivates both by carbon deposition and by framework degradation. However, deactivation by carbon deposition as well as structural damage can be minimized by using optimized reaction conditions of low concentration and temperature and with an alcohol such as methanol as the solvent. The presented work adds to the pool of information regarding this very interesting process wherein it is possible to produce racemic lactic acid or the corresponding methyl ester from biomass-derived substrates. Furthermore, since methyl lactate is formed directly in this process, purification to form high-grade lactic acid could be facilitated by distillation and hydrolysis, thereby avoiding the cumbersome purification process associated with the current production of lactic acid.

Acknowledgments

Supported by the Danish National Research Foundation, and the National Science Foundation, PIRE Program (Award # 0730277). We also thank Dr. J. Rass-Hansen and R. Johansson for technical assistance.

References

[1] R. Dhatta, M. Henry, J. Chem. Technol. Biotechnol. 81 (2006) 1119.
[2] R.A. Sheldon, Green Chem. 7 (2005) 267.
[3] Y.-J. Wee, J.-N. Kim, H.-W. Ryu, Food Technol. Biotechnol. 44 (2) (2006) 163.
[4] R. Leaversuch, Plast. Technol. 48 (3) (2002) 50.
[5] S. Varadarajan, D.J. Miller, Biotechnol. Prog. 15 (1999) 845.
[6] H.F. Shi, Y.C. Hu, Y. Wang, H. Huang, Chin. Chem. Lett. 18 (2007) 476.
[7] R.D. Cortright, M. Sanchez-Castillo, J.A. Dumesic, Appl. Catal. B: Environ. 39 (2002) 353.
[8] J.C. Serrano-Ruiz, J.A. Dumesic, Chem. Sus. Chem. 2 (6) (2009) 581.
[9] D. Garlotta, J. Polym. Environ. 9 (2) (2001) 63.
[10] R.P. John, K.M. Nampoothiri, A. Pandey, Appl. Microbiol. Biotechnol. 74 (2007) 524.
[11] H. Kimura, K. Tsuto, Appl. Catal. A: Gen. 96 (1993) 217.
[12] H. Kimura, Appl. Catal. A: Gen. 105 (1993) 147.
[13] R. Garcia, M. Besson, P. Gallezot, Appl. Catal. A: Gen. 127 (1995) 165.
[14] E. Farnetti, J. Kaspar, C. Crotti, Green Chem. 11 (2009) 704.
[15] D. Hekmat, R. Bauer, V. Neff, Process Biochem. 42 (2007) 71.
[16] S. Yamada, K. Nabe, N. Izuo, M. Wada, I. Chibata, J. Ferment. Technol. 57 (3) (1979) 215.
[17] K. Nabe, N. Izuo, S. Yamada, I. Chibata, Appl. Environ. Microbiol. 38 (6) (1979) 1056.
[18] M.C. Flickinger, D. Perlman, Appl. Environ. Microbiol. 33 (3) (1977) 706.
[19] M.J. Antal Jr., W.S.L. Mok, G.N. Richards, Carbohydr. Res. 199 (1990) 111.
[20] H. Kishida, F. Jin, X. Yan, T. Moriya, H. Enomoto, Carbohydr. Res. 341 (2006) 2619.
[21] M. Bicker, S. Endres, L. Ott, H. Vogel, J. Mol. Catal. A: Chem. 239 (2005) 151.
[22] Y. Hayashi, Y. Sasaki, Chem. Commun. (2005) 2716.
[23] K.P.F. Janssen, J.S. Paul, B.F. Sels, P.A. Jacobs, Stud. Surf. Sci. Catal. 170B (2007) 1222.
[24] E. Taarning, S. Saravanamurugan, M. Spangsberg Holm, J. Xiong, R.W. West, C.H. Christensen, Chem. Sus. Chem. 2 (7) (2009) 625.
[25] S. Sombatchaisak, P. Praserthdam, C. Chaisuk, J. Panpranot, Ind. Eng. Chem. Res. 43 (2004) 4066.
[26] G. Bonn, M. Rinderer, O. Bobleter, J. Carbohydr. Chem. 4 (1) (1985) 67.
[27] B.M. Kabyemela, T. Adschiri, R. Malaluan, K. Arai, Ind. Eng. Chem. Res. 36 (1997) 2025.
[28] G. Lookhart, M.S. Feather, Carbohydr. Res. 60 (1978) 259.
[29] A.C. McLellan, P.J. Thornalley, Anal. Chim. Acta 263 (1992) 137.
[30] C. Rae, S.J. Berners-Price, B.T. Bulliman, P.W. Kuchel, Eur. J. Biochem. 193 (1990) 83.
[31] F. Wakabayashi, J.N. Kondo, K. Domen, C. Hirose, Microporous Mater. 8 (1997) 29.
[32] O. Cairon, T. Chevreau, J.-C. Lavalley, J. Chem., Soc., Faraday Trans. 94 (1998) 3039.
[33] S. Kotrel, J.H. Lunsford, H. Knözinger, J. Phys. Chem. B 105 (2001) 3917.
[34] T. Barzetti, E. Selli, D. Moscotti, L. Forni, J. Chem. Soc. Faraday Trans. 92 (8) (1996) 1401.
[35] C.A. Emeis, J. Catal. 141 (1993) 347.